

## Studies on synthesis of lactic acid and xanthan gum from cheese whey permeate in two phase and three phase moving bed biofilm reactors

C. M. Narayanan<sup>\*,†</sup> and Vikas Narayan<sup>\*\*</sup>

<sup>\*</sup>National Institute of Technology, Durgapur 713209, India

<sup>\*\*</sup>Bangalore, India

(Received 12 February 2021 • Revised 27 March 2021 • Accepted 23 April 2021)

**Abstract**—The performance characteristics of moving-bed biofilm reactors (MBBRs) have been analyzed both mathematically and experimentally. Both two phase operation (lactic acid synthesis from cheese-whey permeate) and three phase operation (Xanthan gum production) in both batch and continuous flow reactors have been studied. Mathematical simulation was performed considering the heterogeneous nature of the system with appropriately defined effectiveness factor being incorporated to account for resistance to substrate transfer into biofilm. The flow reactors were modeled based on the tanks-in-series approach. The mathematical models (software packages) developed were adequately verified by comparing with experimental data. The interesting performance features of these reactors have been highlighted and the dependence of reactor performance on key system/operating parameters such as batch time/space time, catalyst loading and catalyst size has been well-illustrated. The limitation that these bioreactors are best suited mainly for small capacity installations has also been indicated.

Keywords: Moving Bed Biofilm Reactors, Lactic Acid and Xanthan Gum Synthesis, Batch and Flow Reactors, Two Phase and Three Phase Operations, Mathematical Simulation, Tanks-in-series Model

### INTRODUCTION

Moving bed biofilm reactors are relatively simple to build and operate. They also demand low operating cost. However, their major limitation is that they are restricted to low capacity installations. These are heterogeneous reactors that employ support particles (carrier particles) such as silica granules, polymer beads and activated carbon particles. These particles are soaked in microbial solution and the microbial cells are allowed to grow and multiply while remaining in contact with the particle surface (attached growth). As a result, a thin, slimy biofilm gets formed around each particle and these particle - biofilm aggregates remain submerged in the substrate solution inside the reactor (see Figs. 1, 2). They are kept in suspension by agitating with a mechanical impeller or by passing compressed air from below (in case of three phase operation) or by both.

They are called moving bed reactors, though this is a slightly misleading terminology because the particle-biofilm aggregates (discrete phase) are free to move within the liquid bulk, unlike in a packed bed reactor in which the particles are stationary and are in contact with each other. The bioconversion occurs chiefly in the biofilm, where the concentration of microbial cells (cell mass concentration,  $x_f$ ) is substantially large, which helps in attaining high rate of bioconversion. Though the microbial cells grow and multiply within the biofilm, when the thickness of the biofilm ( $\delta$ ) increases beyond a particular limit, the film gets detached from the particle

surface and falls into the liquid bulk, to be replaced by a fresh biofilm, almost instantaneously. This phenomenon is termed as “*sloughing*.” Due to the sloughing phenomenon, the thickness of the biofilm ( $\delta$ ) remains more or less constant throughout the process (usually,  $\delta=0.3-0.4$  mm). The cell mass concentration in the biofilm ( $x_f$ ) also remains essentially constant, due to the same reason.

Moving bed biofilm reactors may be operated batch (Fig. 1) or continuous (Fig. 2). Both two phase (Fig. 2) and three phase (Fig. 1) operations are possible. However, as stated earlier, the reactor vessels employed are of low volume, as these reactors are not economical to use at high capacity, as compared to fluidized bed, semi-

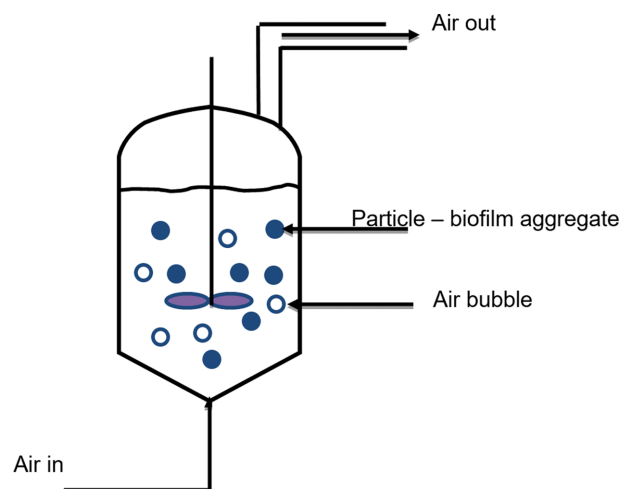


Fig. 1. Moving bed biofilm reactor (batch, three phase).

<sup>†</sup>To whom correspondence should be addressed.

E-mail: prof.cmn@gmail.com

Copyright by The Korean Institute of Chemical Engineers.

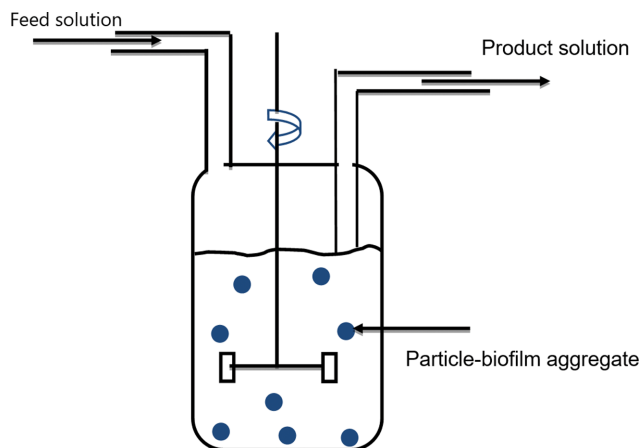


Fig. 2. Moving bed biofilm reactor (continuous, two phase).

fluidized bed and inverse fluidized bed reactors.

Most of the studies reported in the literature on moving bed biofilm reactors deal with wastewater treatment and most of them report laboratory experimental data.

The literature on the basic performance of features of MBBRs and their specific advantages has been briefly surveyed and summarized by Ødegaard [1] and also by McQuarrie and Boltz [2]. One of the earliest experimental studies on these reactors is that of Rusten et al. [3] who reported encouraging results when a moving bed biofilm reactor employing plastic beads as biofilm carriers was used for treating wastewaters from pulp and paper industry. The wastewaters tested were paper mill effluent, bleachery effluent, NSSC effluent and a mixture of CTMP and ground wood effluents.

Studies on nitrification of municipal wastewater in moving bed biofilm reactors have been reported by Hem et al. [4] and Rusten et al. [5]. They used free floating plastic elements as biofilm carriers and conducted studies on nitrification of pre-precipitated wastewater in a once-through system and raw wastewater in a recycled system with pre-denitrification. The observation is that nitrification rate is 20-25% higher with the former (pre-precipitated wastewater without recycle).

Denitrification of wastewater in MBBRs has been experimentally investigated by several authors. Examples are studies reported by Maurer et al. [6], Rusten et al. [7] and also by Szatkowska et al. [8]. Maurer et al. [6] used foam cubes and plastic tubes as biofilm carriers and reported an average denitrification rate of 240 gm per  $m^3$  per day with municipal wastewater at 10 °C. Around 37% of influent COD was reportedly denitrified when the volumetric loading rate to the anoxic reactor was 2.2 kg COD per  $m^3$  per day.

Rusten et al. [7] studied nitrogen removal from dilute wastewater at low temperature (7 to 18 °C). They observed that in the case of pre-denitrification of raw (untreated) wastewater, only 50-70% of total N could be removed at a recirculation ratio of 2.0 and hydraulic residence time 6.0 hours. However, in the case of post-denitrification of pre-precipitated wastewater with acetate as the external carbon source, 80-90% denitrification could be accomplished at a hydraulic residence time of less than 3.0 hours.

Szatkowska et al. [8] used a moving bed biofilm reactor (with Kaldnes rings as carriers for biofilm growth) as a one stage system

for nitrogen removal employing simultaneous partial nitritation and Anammox processes. They observed a nitrogen removal rate of 1.5-1.9 g N per  $m^2$  per day in the pilot plant. In the batch tests, a nitrogen removal rate of 5.2 g N per  $m^2$  per day was observed to be possible when the Anammox process was stimulated by the addition of nitrite.

The use of an MBBR cascade consisting of three to four reactors each operating in a different mode such as in the anaerobic, anoxic or aerobic mode has also been investigated by different authors. All the three processes such as BOD destruction, nitrification and denitrification could be carried out in such a cascade. Kermani et al. [9,10] used three moving bed biofilm reactors in a cascade, the first operating in the anaerobic mode, the second in the anoxic mode and the third in the aerobic mode, for the removal of biological organics and nutrients from municipal wastewater. They reported that 96.9% SCOD removal, 84.6% total nitrogen removal and 95.8% phosphorus removal could be achieved in such a cascade.

In a similar way, Chen et al. [11] employed an anaerobic-aerobic combination of MBBRs for the treatment of landfill leachate. Their experimental results demonstrated that more than 91% COD removal could be achieved at an organic loading of 4.08 kg COD ( $m^3 \cdot d$ ) in the anaerobic MBBR and more than 97% removal of ammoniacal nitrogen was obtained in the aerobic MBBR at a hydraulic retention time of 1.25 days. The system also exhibited strong tolerance to shock loading.

Sahariah et al. [12] also experimented on an aerobic-anoxic-anaerobic combination of MBBRs for handling coke oven wastewater that had been spiked with synthetic pollutants such as phenol, thiocyanate, pyridine and cresols in advance, and found that the anaerobic MBBR could contribute to only 2-5% removal of phenol and around 2% of COD, while the anoxic and aerobic MBBRs could affect 85% removal of thiocyanate, 88% removal of cresols and more than 48% removal of pyridine, along with the residual phenol and COD. The hydraulic retention time maintained was 6.0 days. The anoxic tank could provide more than 94% denitrification and the aerobic tank 64-71% ammonia - N removal.

Studies on dephenolization of wastewater in moving bed biofilm reactors have also yielded encouraging results. Anandkumar et al. [13] reported that up to 98% removal of 4-bromophenol is possible from wastewater samples in an MBBR cascade composed of three reactors operating in the anaerobic-anoxic-aerobic mode. Such a scheme also reportedly affects up to 85% COD removal.

As stated earlier, the majority of the studies were performed on laboratory bench scale and with reference to wastewater treatment. Little attempt was made to mathematically simulate the reactor performance and to develop CAD software packages for the design and analysis of industrial MBBRs.

In the present study, synthesis of lactic acid and Xanthan gum from cheese whey permeate in moving bed biofilm reactors has been analyzed. Cheese whey is the mother liquor left behind after the separation of fats (casein) from milk and is often discharged as a waste effluent. The whey is first passed through an ultrafiltration module to separate all proteins and the permeate (that is free from fats and proteins) is used as the feedstock for the synthesis of lactic acid and Xanthan gum. Lactic acid is synthesized by the micro-

bial fermentation of cheese whey using a culture of *Lactobacillus helveticus*, while Xanthan gum synthesis employs a culture of *Xanthomonas campestris*, which are aerobic microbes. In both cases, lactose present in cheese whey is the principal substrate that gets converted to either lactic acid or to Xanthan gum by the action of the respective microbes. Lactic acid synthesis is a two phase process, while Xanthan gum synthesis involves a three phase (gas-liquid-solid) system.

Lactic acid is the starting material (monomer) for the synthesis of the popular bioplastic, PLLA (Poly laevo lactic acid). Xanthan gum is widely used as an emulsifying and stabilizing agent in many food and dairy industries.

Lactic acid synthesis from molasses and cheese whey permeate in fluidized bed biofilm reactors was studied by Narayanan [14], that in semifluidized bed biofilm reactors and inverse fluidized bed biofilm reactors by Narayanan and Das [15,16]. Performance characteristics of these bioreactors in this connection have been reported to be truly encouraging. Typically, a fluidized bed biofilm reactor of expanded bed height 3.15 m (column diameter=0.5 m) composed of 2.5 mm support particles (biofilm thickness=0.3 mm) has been found to provide 77% conversion of whey lactose to lactic acid at a feed flow rate of 7,200 L/hr, while a semifluidized bed biofilm reactor of total height 1.0 m (same column diameter, same size of support particles) reportedly provides 82.6% conversion of lactose, when operated at much larger feed flow rate of 79,000 L/hr. In comparison, an inverse fluidized biofilm reactor of same column diameter, but of inverse fluidized bed height=2.4 m and composed of larger size (12.5 mm) support particles, provides 76% conversion of lactose at a capacity of 59,000 L/hr.

In fluidized bed bioreactors, the substrate conversion increases with increase in feed flow rate, due to increase in bed height and consequent increase in reactor volume; and once fully fluidized, the pressure drop across the bed remains essentially constant and does not increase with increase in feed flow rate. These are their distinct advantages. Semifluidized bed bioreactors, on the other hand, provide high degree of substrate conversion even when operated at much higher capacity (feed flow rate) and in this case also, the substrate conversion increases with increase in feed flow rate, even though the total height of semifluidized bed remains constant. This is due to the re-arrangement of reaction zones within the reactor: the height of the packed section increasing and that of the fluidized section proportionally decreasing with increase in feed flow rate. The operating cost of these bioreactors is nevertheless higher.

Due to their downflow mode of operation, the inverse fluidized bed bioreactors possess low operating cost and permit use of large size support particles (12.5 mm and above). They provide reasonably high substrate conversion at moderately high reactor capacity.

Studies on lactic acid production from molasses and cheese whey permeate in downflow stationary fixed film (DSFF) bioreactors have been reported by Pandey and Narayanan [17,18]. DSFF bioreactors also employ downflow mode of operation and thus are of low operating cost. They provide satisfactory performance at reasonably high capacity, when multichannel construction is employed. These reactors, however, demand relatively large reactor volume.

Synthesis of Xanthan gum from cheese whey permeate in three phase semifluidized bed biofilm reactors was investigated by Nara-

yanan [19]. Here also, more than 85% conversion of lactose to Xanthan gum has been reported to be possible in an aerobic semifluidized bed biofilm reactor of height 1.0 m, at feed flow rates exceeding 85,000 L/hr.

## MATHEMATICAL MODELING AND SIMULATION OF BIOREACTOR PERFORMANCE

The performance characteristics of both batch and continuous moving bed biofilm reactors, handling two phase system (lactic acid synthesis) as well as three phase system (Xanthan gum synthesis) have been analyzed mathematically and versatile simulation models (software packages) have been developed. These are summarized below.

### 1. Lactic Acid Synthesis from Cheese Whey Permeate in Two Phase Moving Bed Biofilm Batch Reactor

When operated batchwise, the bioreactor is composed of an agitated vessel containing the particle-biofilm aggregates--in this case silica granules each surrounded by a thin biofilm of *Lactobacillus helveticus*--suspended in the substrate solution; in this case, cheese whey permeate that has been diluted to a lactose concentration of 9 g/L. Due to the agitation provided by the mechanical impeller, the particle-biofilm aggregates get more or less uniformly distributed in the liquid bulk and remain submerged in the substrate solution. The system is thus the same as that shown in Fig. 1, except that there is no supply of air from the bottom and, as a result, there are no air bubbles present in the reaction mixture.

Reported studies [20] have demonstrated that bioconversion of lactose to lactic acid by *Lactobacillus helveticus* intrinsically follows a Monod-type kinetic equation:

$$(-r_s)(\text{int}) = (\mu_m/Y) \times C_s / [K_s + C_s] \quad (1)$$

Typical experimental values of kinetic constants and the yield coefficient are [20],

$$\begin{aligned} \mu_m &= 0.7 \text{ hr}^{-1} \\ K_s &= 0.22 \text{ g/L} \\ Y &= 0.65 \end{aligned} \quad (2)$$

The above equation is based on suspended growth of microbes. For attached growth of microbes that occur in the present reactor, the above equation for intrinsic rate gets modified to

$$(-r_s)(\text{int}) = \mu_m(\text{app}) C_s / [K_s + C_s] \quad (3)$$

$$\text{where } \mu_m(\text{app}) = (\mu_m/Y) x_f f \varepsilon / (1 - \varepsilon) \quad (4)$$

$x_f$  = cell mass concentration in the biofilm

$\varepsilon$  = volume fraction of particle - biofilm aggregates in the reaction mixture

$f$  = volume fraction of biofilm in particle - biofilm aggregate

$$= 1 - (d_p/d_{pm})^3 \quad (5)$$

$d_p$  = diameter of each support particle (silica granule)

$d_{pm}$  = diameter of each particle - biofilm aggregate

$$= (d_p + 2\delta) \quad (6)$$

$\delta$  = average thickness of biofilm (assumed constant)

As stated earlier, the average thickness of each biofilm ( $\delta$ ) remains constant throughout the process and is of the order of 0.3-0.4 mm. Since the tank volume (reactor volume) is low, it is not too erroneous to assume the performance of the bioreactor to be more or less equivalent to an ideal batch reactor. In other words, though the substrate concentration ( $C_s$ ) does change with time, it is assumed that it does not vary from one point to another within the reaction mixture at any time  $t$ . This is achieved by adequately selecting the agitator speed (and agitator dimensions) and thereby ensuring that the particle-biofilm aggregates are uniformly dispersed within the solution bulk. Based on this approach, the performance equation for the bioreactor is

$$(-dC_s/dt) = \eta(-r_s)(int) \tag{7}$$

where  $\eta$ =effectiveness factor (computation of which is discussed subsequently)

Substituting the expression for intrinsic rate from Eq. (3) and rearranging, we get

$$t = \tau = \int_{C_{se}}^{C_{s0}} F(C_s) dC_s \tag{8}$$

where  $F(C_s) = (K_s + C_s) / [\eta \mu_m (app) C_s]$  (9)

$\tau$ =batch time

$C_{s0}$ =initial concentration of lactose in substrate solution (at  $t=0$ )

$C_{se}$ =concentration of lactose in substrate solution at  $t = \tau$

The effectiveness factor ( $\eta$ ) that accounts for the resistance to substrate transfer into the biofilm is a function of the characteristic dimension of the particle-biofilm aggregate ( $L^*$ ), the effective diffusivity of substrate (lactose) into the biofilm ( $D_e$ ) and the kinetic constants ( $\mu_m (app)$  and  $K_s$ ). For bioconversion processes that intrinsically follow Monod - type kinetic equation such as the one under consideration, a reasonable estimate of  $\eta$  could be obtained from the correlation proposed by Gottifreddi and Gonzo [21], which is reproduced below:

$$(1/\eta)^2 = (1/\eta_d)^2 + \exp[\Phi_b - (1/\eta_d)^2] \tag{10}$$

where  $\Phi_b = 6\Phi^2 / \{5(1+\beta)^2\}$  (11)

$$\Phi = L^* \sqrt{\mu_m (app) / (D_e K_s)} \tag{12}$$

$$L^* = (d_{pm}^3 - d_p^3) / (6d_{pm}^2) \tag{13}$$

$$\beta = (C_s / K_s) \tag{14}$$

$$\eta_d = (\sqrt{2}/\Phi) ((1+\beta)/\beta) \sqrt{\beta - \ln(1+\beta)} \tag{15}$$

After substituting Eq. (9) in Eq. (8), it can be integrated numerically using Simpson's rule, or any other appropriate algorithm, with the help of Eqs. (10) to (15), to estimate the batch time ( $\tau$ ) required for attaining any specified fractional substrate conversion ( $\alpha$ ), where  $\alpha$  is defined as

$$\alpha = (C_{s0} - C_{se}) / C_{s0} \tag{16}$$

If the rate of lactic acid synthesis desired is  $M$  kg/hr, then the volume of reactor required will be

$$V = (M\tau) / [4C_{s0}\alpha(1-\epsilon)(M_p/M_A)] \tag{17}$$

where  $M_p, M_A$ =molecular weight of lactic acid and that of lactose, respectively

$\alpha$ =fractional substrate conversion attained in a batch time of  $\tau$  hours

To note that as per stoichiometry, one mole of lactose yields four moles of lactic acid on complete conversion.

The performance characteristics of such a batch - operated moving bed biofilm reactor with respect to lactic acid synthesis are illustrated and discussed in the subsequent section on Results and Discussion. The discussion is based on the results from the above mathematical model and the elaborate experimental data compiled.

### 2. Xanthan Gum Synthesis from Cheese Whey Permeate in Three Phase Moving Bed Biofilm Batch Reactor

As stated earlier, bioconversion of lactose, present in cheese whey permeate, into Xanthan gum is an aerobic process. The microbial culture employed is that of *Xanthomonas campestris*. The bioreactor is that presented in Fig. 1. The operation is batchwise and air is sparged continuously from the bottom throughout the period of operation. It can be safely assumed that air moves up in the form of very tiny bubbles and a dispersed flow regime exists within the reactor. Thus, these tiny bubbles of air are well dispersed and do not disturb the biofilm or the particle - biofilm aggregates that remain suspended in the substrate solution. Being a three phase system, we have to account for the gas holdup ( $\epsilon_g$ ) in the reactor as well; the magnitude  $\epsilon_g$  will be relatively low in most cases though. Experimental correlations for the estimation of gas holdup in three phase agitated vessels have been proposed by several authors. Examples are those proposed by Dohi et al. [22], Bao et al. [23], Rapala and Karcz [24,25] and Godlewska and Karcz [26]. All of these correlations are highly empirical and are applicable only within a specific range of operating/system parameters (tank and impeller dimensions, impeller speed, solid concentration, gas velocity) utilized in the experiments. The most suitable correlation for a given application can be thus selected only by trial and exercising great caution. In the present case, the correlation proposed by Godlewska and Karcz [26] has been observed to predict reliable estimates of fractional gas holdup in the bioreactor. Their correlation is reproduced below:

$$\epsilon_g = 0.00383 (P_{gl}/V)^{0.521} (U_g)^{0.185} (X)^{0.0169} \tag{18}$$

where  $X$ =mass fraction of solids (particle - biofilm aggregates) in the reaction mixture.

The power input per unit volume, ( $P_{gl}/V$ ), can be estimated from the correlation reported by Patrick and Kennedy [27] and is given below :

$$P_{gl}/V = [1.26P_{gl}] - [X(\rho_{sm}/\rho_L)^{6.9}] \tag{19}$$

where  $P_{gl}$ =power consumption for a gassed liquid (20)  
 $= [P_L^2 n D_a^5 / Q_g^{0.53} Q_g^{0.43}]$

$P_L$ =power consumption for an ungassed liquid (21)  
 $= (K_T n^3 D_a^5 \rho_L)$ , for  $Re_m \geq 10,000$

$Re_m$ =mixing Reynolds number =  $[n D_a^2 \rho_L / \mu_L]$  (22)

$\rho_{sm}$ =density of each particle - biofilm aggregate (22a)  
 $= f\rho_m + (1-f)\rho_s$

$\rho_s, \rho_m$  = density of support particle (silica granule) and that of microbial solution, respectively

When the impeller is operating in the fully developed turbulent zone ( $Re_m \geq 10,000$ ), the power number (Po) remains more or less constant (will become independent of  $Re_m$ ) and will be equal to  $K_T$  (called the turbulent constant). Typically,  $K_T = 6.3$  for a six bladed turbine (Rushton impeller) operating in a baffled tank.

The value of  $P_{gLS}$  can be computed from the correlation proposed by Rapala and Karcz [24] as well. According to them,

$$(P_{gLS}/V) = (45.8 X + 0.926) [1.0 - (0.229 + 11.71 X) (60Q_g/V)] (\rho_L) \quad (23)$$

However, the above correlation is strictly valid to those cases in which the impeller is operating at its critical speed, which is given by

$$n(\text{critical}) = (48.8 X + 4.296) [1.0 + (0.223 - 0.08 X) (60Q_g/V)] \quad (24)$$

By critical speed, we mean the minimum speed (rpm) of the impeller required to uniformly disperse the solid particles and gas bubbles in the liquid bulk. Incidentally, in the present case, the values of power input per unit volume computed from correlations (19) and (23) do not differ significantly.

As in the case of lactic acid synthesis, in this case also, it may be assumed with allowable error that the bioreactor performs more or less equivalent to an ideal batch reactor and accordingly, the performance equation of the reactor will be same as that given in Eq. (7). Zabet et al. [28] have reported that bioconversion of cheese whey lactose into Xanthan gum using *X. Campestris* culture intrinsically follows Contois-type kinetic equation. Thus

$$(-r_s)(\text{int}) = (\mu_m/Y) x C_s / [K_c x + C_s] \quad (25)$$

where  $K_c$  = Contois kinetic constant, dimensionless

Since attached growth of microbes occurs in the present reactor, the above equation is to be rewritten as

$$(-r_s)(\text{int}) = \mu_m(\text{app}) C_s / [K_c(\text{app}) + C_s] \quad (26)$$

where  $\mu_m(\text{app}) = (\mu_m/Y) x_f \varepsilon / (1 - \varepsilon - \varepsilon_s)$  (27)

$$K_c(\text{app}) = (K_c x_f \varepsilon) / (1 - \varepsilon - \varepsilon_s) \quad (28)$$

Typical values of kinetic constants reported by Zabet et al. [28] are,

$$\begin{aligned} \mu_m &= 0.29 \text{ hr}^{-1} \\ K_c &= 2.0 \\ Y &= 0.5 \end{aligned} \quad (29)$$

After substituting the above kinetic equation in Eq. (7) and rearranging, we get

$$t = \tau = \int_{C_{se}}^{C_{s0}} G(C_s) dC_s \quad (30)$$

where  $G(C_s) = (K_c(\text{app}) + C_s) / [\eta \mu_m(\text{app}) C_s]$  (31)

The values of the effectiveness factor ( $\eta$ ) can be computed from Eq. (10) itself, except that the kinetic constant  $K_s$  is to be replaced by  $K_c(\text{app})$ . Thus

$$\phi = L \sqrt{\mu_m(\text{app}) / [D_e K_c(\text{app})]} \quad (32)$$

$$\beta = C_s / K_c(\text{app}) \quad (33)$$

The batch time ( $\tau$ ) required to attain a given fractional substrate conversion ( $\alpha$ ) can be now estimated through numerical integration of Eq. (30) with the help of Eqs. (10), (15), (32) and (33).

The performance characteristics of this bioreactor are also illustrated graphically and discussed in the subsequent section on Results and Discussion. In this case also, it has been observed that there is good agreement between the experimental data compiled and the results computed from the above mathematical model.

### 3. Continuous Moving Bed Biofilm Reactor (Two Phase) for Lactic Acid Synthesis

When used as a continuous flow reactor, the moving bed biofilm reactor resembles a CSTR (continuous stirred tank reactor), except that the reaction mixture is now composed of two phases. The feed solution (cheese whey permeate) is admitted from the top and the product solution (composed mainly of lactic acid) also leaves from the top (see Fig. 2). Bottom discharge of product solution simulates discharge of particle - biofilm aggregates along with the product solution and this tends to disturb the overall stability of reactor operation.

Since the reactor employs a tank of relatively low volume, the performance of the bioreactor may be approximated to that of an ideal CSTR (backmix reactor), but with a heterogeneous (multi-phase) reaction mixture. However, it is more accurate to assume the bioreactor is equivalent to three ideal CSTRs, each of volume  $V/3$ , in series. This is termed as the "tanks-in-series-model" and it has been observed to provide more reliable predictions on the reactor performance. Based on this model, the performance equation for the first backmix reactor in the cascade is

$$\tau = (C_{s0} - C_{s1}) / [\eta (-r_{s1})(\text{int})] \quad (34)$$

where  $\tau$  = space time of the reactor =  $[V(1 - \varepsilon) / 3Q_0]$  (35)

$C_{s1}$  = concentration of substrate (lactose) in the product solution leaving the reactor

$Q_0$  = volume flow rate of feed solution entering the reactor

Substituting the expression for intrinsic rate from Eq. (3) and rearranging, we get

$$\tau = (C_{s0} - C_{s1})(K_s + C_{s1}) / [\eta \mu_m(\text{app}) C_{s1}] \quad (36)$$

or  $(C_{s1})^2 + [K_s - C_{s0} + \eta \tau \mu_m(\text{app})] C_{s1} - (K_s C_{s0}) = 0$  (37)

where  $\mu_m(\text{app})$  is the clubbed kinetic constant defined in Eq. (4). The value of effectiveness factor ( $\eta$ ) is to be computed from Eqs. (10) to (15) after substituting  $C_s = C_{s1}$ . In a similar way, for the second reactor (reactor 2) of the cascade,

$$(C_{s2})^2 + [K_s - C_{s1} + \eta \tau \mu_m(\text{app})] C_{s2} - (K_s C_{s1}) = 0 \quad (38)$$

And finally for the last reactor (reactor 3),

$$(C_{se})^2 + [K_s - C_{s2} + \eta \tau \mu_m(\text{app})] C_{se} - (K_s C_{s2}) = 0 \quad (39)$$

We have assumed a constant density system such that the volumetric flow rate of the substrate solution flowing from one reactor to another could be assumed to remain more or less constant at  $Q_0 \text{ m}^3/\text{s}$ . At a specified value of reactor space time ( $\tau$ ), the above three equations, such as Eqs. (37), (38) and (39), are solved simultaneously to obtain the value of  $C_{se}$  (lactose concentration in the

final product solution) and thereby estimate the fractional substrate conversion attained ( $\alpha$ ). However, the solution demands a trial and error procedure. For example, Eq. (37) is solved for  $C_{S1}$  by trial, as given below:

(i) First, a value of  $C_{S1}$  is assumed. For example, let

$$C_{S1} = (C_{S0} - 1.0) \text{ g/L} \quad (40)$$

(ii) Put  $X = C_{S1}$ .

(iii) The value of effectiveness factor ( $\eta$ ) at  $C_S = C_{S1}$  is then computed from Eqs. (10) to (15).

(iv) Eq. (27) is now solved for  $C_{S1}$  (Note that it is a quadratic equation in  $C_{S1}$ ).

(v) The fractional deviation is computed as,

$$\sigma = (X - C_{S1}) / C_{S1} \quad (41)$$

(vi) If the magnitude of fractional deviation ( $\sigma$ ) is found to be significantly large, the computations are repeated starting from step (ii).

In a similar way, Eq. (38) is solved by trial for  $C_{S2}$  and, finally, the value of  $C_{Se}$  is estimated from Eq. (39) by following the same trial and error procedure. The value of fractional substrate conversion ( $\alpha$ ) is then computed from Eq. (16) given earlier. Note that this value of substrate conversion corresponds to a reactor space time,  $\tau$  (or, a bioreactor of volume  $V$ , operating at a feed flow rate  $Q_0$ ) and a solid concentration (catalyst concentration),  $\varepsilon$ . The algorithm is re-executed at different values of operating/system parameters such as the feed flow rate ( $Q_0$ ), catalyst concentration ( $\varepsilon$ ) and the total volume of reaction mixture ( $V$ ), and the results are illustrated graphically in the subsequent section on Results and Discussion. The comparison between the experimental values of  $\alpha$  and those computed from the above - described mathematical model is illustrated in the next section on Experimental Study.

#### 4. Continuous Three Phase Moving Bed Biofilm Reactor for Xanthan Gum Synthesis

In three phase continuous mode of operation, the moving bed biofilm reactor resembles an aerobic tank of the activated sludge process, with the difference that the substrate solution (cheese whey permeate) inside the reactor consists of suspended biocatalyst particles (particle - biofilm aggregates) as well. The schematic of the bioreactor is therefore the same as that sketched in Fig. 2, except that air is being sparged continuously into the reactor tank from the bottom and it moves up through the liquid bulk in the form of tiny, dispersed bubbles.

In this case also, it is observed that the bioreactor can be modeled based on the tanks - in - series concept, with  $n$  = number of small reactors in the cascade = 3. So, the bioreactor may be assumed as equivalent to an ideal CSTR cascade composed of three reactors in series (active volume of each reactor =  $V/3$ ). Accordingly, the performance equation of each backmix reactor in the cascade is that given in Eq. (34). If we substitute the expression for intrinsic rate from Eq. (26) and rearrange, we get

$$\tau = (C_{S0} - C_S)(K_C(\text{app}) + C_S) / [\eta \mu_m(\text{app}) C_S] \quad (42)$$

$$\text{or } (C_S)^2 + [K_C(\text{app}) - C_{S0} + \eta \tau \mu_m(\text{app})] C_S - (K_C(\text{app}) C_{S0}) = 0 \quad (43)$$

$$\text{where } \tau = \text{space time} = [V(1 - \varepsilon - \varepsilon_g) / 3Q_0] \quad (44)$$

The kinetic constants  $\mu_m(\text{app})$ ,  $K_C(\text{app})$  are those defined in Eqs. (27) and (28), respectively. The value of fractional gas holdup ( $\varepsilon_g$ ) is to be estimated from Eqs. (18) to (22) given in the earlier section. The effectiveness factor ( $\eta$ ) is evaluated from Eqs. (10), (15), (32) and (33).

The above performance equation, Eq. (43), can be written separately for each reactor of the cascade (in a similar way as is shown in Section 4). Thus, for reactor 1 of the cascade,

$$(C_{S1})^2 + [K_C(\text{app}) - C_{S0} + \eta \tau \mu_m(\text{app})] C_{S1} - (K_C(\text{app}) C_{S0}) = 0 \quad (45)$$

For reactor 2,

$$(C_{S2})^2 + [K_C(\text{app}) - C_{S1} + \eta \tau \mu_m(\text{app})] C_{S2} - (K_C(\text{app}) C_{S1}) = 0 \quad (46)$$

And for the last reactor (reactor 3),

$$(C_{Se})^2 + [K_C(\text{app}) - C_{S2} + \eta \tau \mu_m(\text{app})] C_{Se} - (K_C(\text{app}) C_{S2}) = 0 \quad (47)$$

The above three equations are solved successively using the trial and error procedure outlined in the earlier section to obtain the value of substrate concentration (concentration of unreacted lactose) in the final product solution ( $C_{Se}$ ) at the specified value of reactor space time ( $\tau$ ). The fractional substrate conversion attained ( $\alpha$ ) is then computed from Eq. (16).

The algorithm is executed at different values of feed flow rate,  $Q_0$ , which decides the reactor capacity, and at different values of catalyst loading ( $\varepsilon$ ). The results are illustrated graphically in the subsequent section on Results and Discussion. The experimental verification of the above mathematical model is presented in the next section.

## EXPERIMENTAL STUDY (MATERIALS AND METHODS)

All the developed mathematical models described in the earlier sections have been tested and verified by comparing the results derived from these models (software packages) with elaborate experimental data compiled on laboratory batch and continuous bioreactors (MBBRs).

### 1. Batch Two Phase MBBR (Lactic Acid Synthesis)

Experiments were conducted in a batch moving bed biofilm reactor of diameter 0.8 m ( $D=0.8$  m), height 1.0 m and agitated with a 500 rpm Rushton impeller ( $D_a=D/3$ ). 1.0 mm silica granules were used as the support media for biofilm growth. Clarified cheese whey permeate diluted to a lactose concentration of 9.0 g/L, by adding demineralized water, was used as the substrate solution. Volume fraction of solids (particle-biofilm aggregates) in the slurry was maintained at 0.02 (2.0%). Samples of solution were collected at regular intervals of time and analyzed for lactose content using a precalibrated spectrophotometer (at 800 nm wave length). The values of fractional substrate conversion attained ( $\alpha$ ) at different values of batch time ( $\tau$ ) were thus estimated. The experimental runs were repeated at least thrice to ascertain the accuracy of the measurements made.

The comparison between the experimental values of  $\alpha$  and those computed from the mathematical model described in the earlier section is illustrated and discussed in the next section on Results and

Discussion.

## 2. Batch Three Phase MBBR (Xanthan Gum Synthesis)

The bioreactor (stirred tank) of the same dimensions as above was used here. 1.0 mm silica granules soaked with the microbial culture of *Xanthomonas campestris* were mixed with clarified cheese whey permeate (whose lactose content= $C_{s0}=9.0$  g/L), such that the mass fraction of solids in the slurry=0.03 and agitated using the Rushton impeller operating at 500 rpm. Since the process is aerobic, compressed air was sparged from the bottom of the reactor at a steady rate of 7,200 L/hr. Samples of substrate solution (containing partly converted lactose and lactic acid) were collected at specific intervals of time and the lactose content of each sample was determined using the pre-calibrated spectrophotometer. The  $\alpha$  values were estimated from Eq. (16) from the data compiled.

The above results were now compared with  $\alpha$  values computed based on the mathematical model outlined in the earlier section and the comparison is discussed in the next section (see Fig. 4).

## 3. Continuous Operation of Two Phase MBBR (Lactic Acid Synthesis)

In the case of continuous operation, a bioreactor of larger diameter ( $D=1.0$  m) and larger height ( $H=1.5$  m) was used. The clarified cheese whey permeate (lactose content=9.0 g/L) was pumped at a specific flow rate ( $Q_0$ ) into the reactor tank and the reaction mixture was agitated using the Rushton impeller to ensure that all the particle - biofilm aggregates (1.0 mm silica granules each surrounded by a thin biofilm of *Lactobacillus helveticus*) remained uniformly suspended in the liquid bulk. The product solution was made to overflow out at the same flow rate, the flow rates being recorded using pre-calibrated rotameters. The mass fraction of solids (particle - biofilm aggregates) in the reaction mixture was maintained at 0.03. Once the system attained steady state (once the concentration of unconverted lactose in the exit stream,  $C_{se}$ , remained more or less constant), the lactose concentration ( $C_{se}$ ) was recorded using the pre-calibrated spectrophotometer. The experimental runs were repeated at different values of feed flow rate ( $Q_0=0.35$  to  $0.50$  m<sup>3</sup>/h) and in each case, the steady state value of  $C_{se}$  was recorded. Since  $C_{s0}=9.0$  g/L, the value of  $\alpha$  (fractional conversion of lactose to lactic acid) at each was computed from Eq. (16).

The experimental values of  $\alpha$  so computed were now compared with mathematically estimated values from the software package described in the earlier section and the comparison is presented graphically in Fig. 5 of next section.

## 4. Continuous Three Phase MBBR (Xanthan Gum Synthesis)

The bioreactor was also operated in the three phase, continuous mode to analyze the Xanthan gum production from cheese whey permeate. The operation is similar to that for lactic acid synthesis, except that compressed air is also sparged continuously into the reaction mixture from the bottom at a specified flow rate of 7,200 L/hr (the air flow rate being monitored by a velometer with digital display). The bacterial culture employed is that of *X. campestris*. Here also, sufficient time was provided for the reactor to attain steady state and thereafter the steady state concentration of lactose in the exit stream (product solution) was recorded using the pre-calibrated spectrophotometer.

Experimental runs were repeated by changing the magnitude of the feed flow rate ( $Q_0$ ) and at each value of  $Q_0$ , the steady state value

of  $C_{se}$  was recorded and the fractional substrate conversion ( $\alpha$ ) computed therefrom. Typical results are illustrated graphically in Fig. 6 of next section.

## RESULTS AND DISCUSSION

### 1. Verification of Mathematical Models (Software Packages) Developed (Model Validation)

As stated earlier, the accuracy and reliability of the mathematical models developed are first ascertained by comparing the model results with the experimental data compiled. In the case of two phase, batch MBBR handling lactic acid synthesis, the comparison between the experimental values of  $\alpha$  and those computed from the mathematical model described earlier is shown in Fig. 3. It can be seen that  $\alpha$  (experimental) and  $\alpha$  (computed) agree closely, with a maximum deviation of  $\pm 10\%$ . This confirms the accuracy and applicability of the mathematical model developed.

Comparison between  $\alpha$  values computed and those experimen-

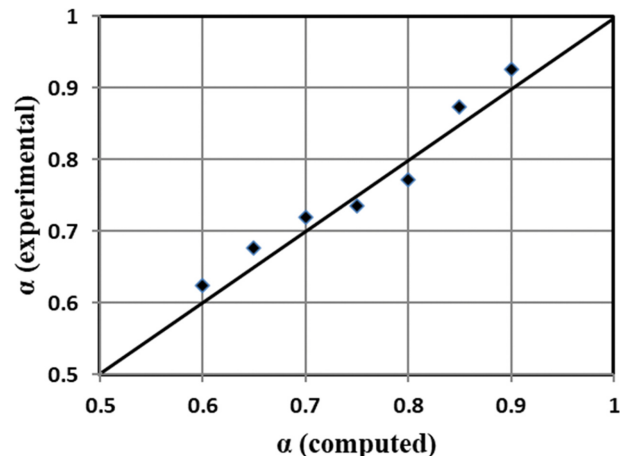


Fig. 3. Comparison between computed and experimental values of fractional lactose conversion,  $\alpha$  (lactic acid synthesis in batch moving bed biofilm reactor).  $d_p=1.0$  mm,  $\varepsilon=0.02$ .

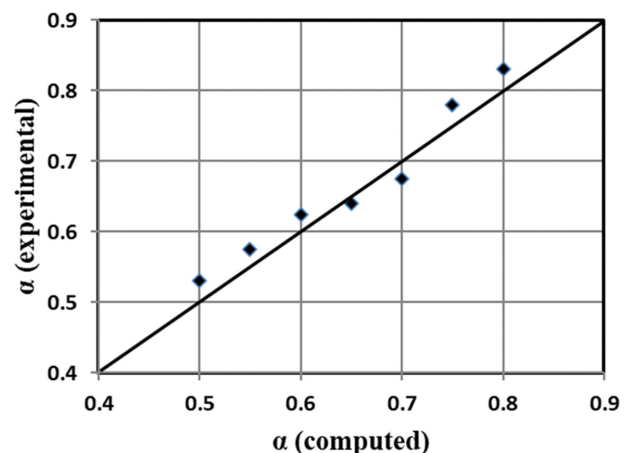


Fig. 4. Comparison between computed and experimental values of fractional substrate conversion,  $\alpha$  (Xanthan gum synthesis in three phase batch moving bed biofilm reactor).

tally determined in the case of three phase, batch MBBR that handles Xanthan gum production from cheese whey permeate is illustrated graphically in Fig. 4. Values of  $\alpha$  have been computed based on the mathematical model outlined earlier. It can be seen from Fig. 4 that in this case also, there is good agreement between  $\alpha$  values computed from the mathematical model and those experimentally determined, the deviation between the two seldom exceeding  $\pm 8\%$ . This once again ascertains the accuracy of the mathematical model developed, which invariably consists of an empirical correlation selected for the computation of fractional gas holdup in the reaction mixture.

For continuous operation of a typical MBBR that handles a two phase system involving lactic acid synthesis, the comparison between computed and experimental values of fractional substrate conversion ( $\alpha$ ) is demonstrated graphically in Fig. 5. The  $\alpha$  values have been computed from the tanks-in-series model and the experimental values have been compiled as described in the earlier section. Here also, satisfactory agreement can be observed between  $\alpha$  (experimental) and  $\alpha$  (computed) and this depicts the reliability of the developed simulation package (based on tanks - in - series model).

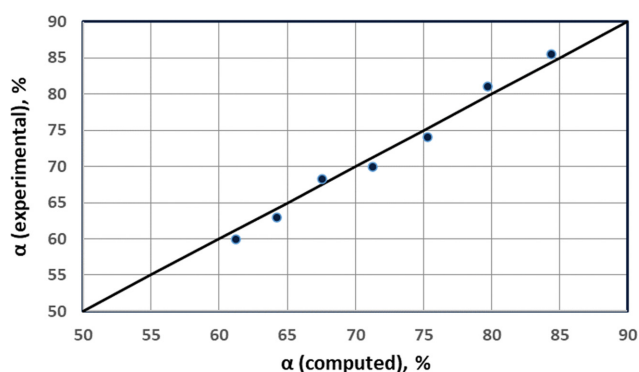


Fig. 5. Comparison between computed and experimental values of fractional lactose conversion,  $\alpha$  (lactic acid synthesis). Continuous moving bed biofilm reactor,  $d_p=1.0$  mm,  $\varepsilon=0.02$ .

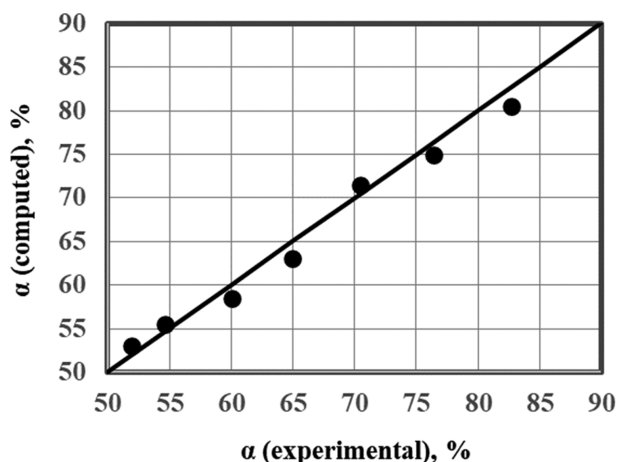


Fig. 6. Comparison between experimental and computed values of fractional substrate conversion ( $\alpha$ ). Continuous operation of three - phase MBBR (Xanthan gum production).  $d_p=1.0$  mm,  $X=0.03$ .

For continuous operation of a three phase MBBR employed for synthesis of Xanthan gum from cheese whey permeate, typical comparison between computed and experimental values of fractional lactose conversion ( $\alpha$ ) is presented in Fig. 6. The computed values of  $\alpha$  are those based on the mathematical model described earlier (tanks-in-series model) and the experimental data compilation is that discussed in the earlier section. In this case also, the agreement between  $\alpha$  (experimental) and  $\alpha$  (computed) is seen to be quite satisfactory, the average percentage deviation being well within 10%.

## 2. Performance of Two Phase Batch MBBR (Lactic Acid Synthesis)

The performance characteristics of the two phase, batch moving bed biofilm reactor dealing with lactic acid synthesis from cheese whey permeate are determined from the well verified mathematical model and are illustrated in Figs. 7 and 8. Fig. 7 displays the variation of fractional substrate conversion ( $\alpha$ ) with the batch time ( $\tau$ ) employed. This plot is for a catalyst loading ( $\varepsilon$ ) of 0.02. The size of support particles ( $d_p$ ) is 1.0 mm. The variation of  $\alpha$  with  $\tau$  can be seen to be more or less linear. Based on a regression analy-

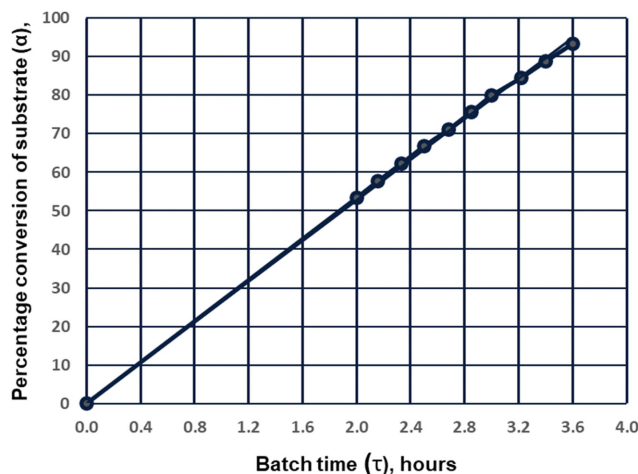


Fig. 7. Plot of fractional substrate conversion ( $\alpha$ ) versus batch time ( $\tau$ ) for batch, two phase MBBR with catalyst loading ( $\varepsilon$ )=0.02, support particle size ( $d_p$ )=1.0 mm.

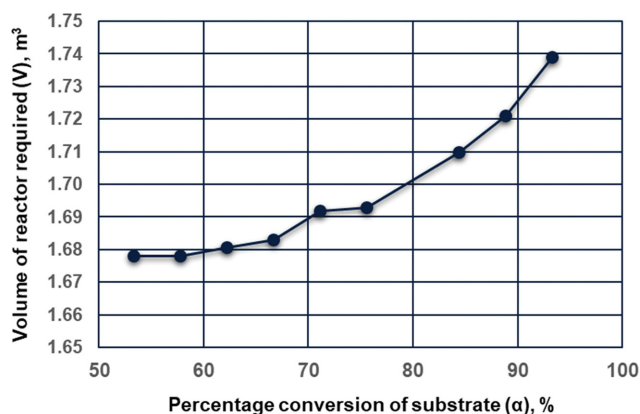


Fig. 8. Plot of volume of reactor required ( $V$ ) versus fractional substrate conversion ( $\alpha$ ) for batch, two phase MBBR with catalyst loading ( $\varepsilon$ )=0.02, support particle size ( $d_p$ )=1.0 mm.

sis,  $\alpha$  could be correlated with  $\tau$  as

$$\alpha = 0.2639\tau \quad (R^2 = 0.999) \quad (48)$$

As a result, the volume of reactor required ( $V$ ), computed from Eq. (17) given earlier, remains more or less constant and varies only marginally with increase in fractional lactose conversion ( $\alpha$ ) or increase in batch time ( $\tau$ ) employed. This is well illustrated in Fig. 8, which corresponds to a desired capacity (rate of production of lactic acid,  $M$ ) of 100 kg/d.

From the above plots, it can be deduced that at a catalyst loading of  $\varepsilon = 0.02$ , more than 90% conversion of whey lactose to lactic acid is possible within around 3.5 hr in a batch MBBR of volume  $1.7 \text{ m}^3$ . The rate of production of lactic acid with such a batch reactor is 100 kg/d and if we employ five such reactors in parallel (which is not uncommon in process industries), the capacity increases to 500 kg/d.

Typical plots illustrating variation of fractional substrate conversion ( $\alpha$ ) with batch time ( $\tau$ ) at a lower value of catalyst loading such as when  $\varepsilon = 0.015$  are shown in Fig. 9. In this case also, the

variation of  $\alpha$  with  $\tau$  is seen to be more or less linear ( $\alpha = 0.1972\tau$ ,  $R^2 = 0.9979$ ). Consequently, the variation of the required volume of the reactor ( $V$ ) at a desired capacity (rate of production of lactic acid) of  $M = 100 \text{ kg/d}$  with  $\alpha$  or  $\tau$  is quite marginal with this value of catalyst loading as well (Fig. 10). However, a lower catalyst loading demands larger batch time ( $\tau$ ) for attaining the desired degree of fractional substrate conversion ( $\alpha$ ). The volume of reactor required ( $V$ ) is also larger. For example, when the catalyst loading ( $\varepsilon$ ) maintained is 0.02, 80% conversion of lactose can be achieved within a batch time of 3.0 hours (Fig. 7), whereas at  $\varepsilon = 0.015$  (Fig. 9), the batch time required to attain the same degree of lactose conversion is around 4.0 hours (33% higher). The volume of reactor required for 100 kg/d of lactic acid production also increases from  $1.7 \text{ m}^3$  to  $2.25 \text{ m}^3$  (see Figs. 8 and 10).

A catalyst loading higher than 0.02 ( $\varepsilon > 0.02$ ) could still reduce the batch time required to attain the desired substrate conversion ( $\alpha$ ). However, at much higher values of  $\varepsilon$  much larger speed of agitation will be required to keep all the particle-biofilm aggregates in suspension and uniformly distributed within the liquid bulk. At

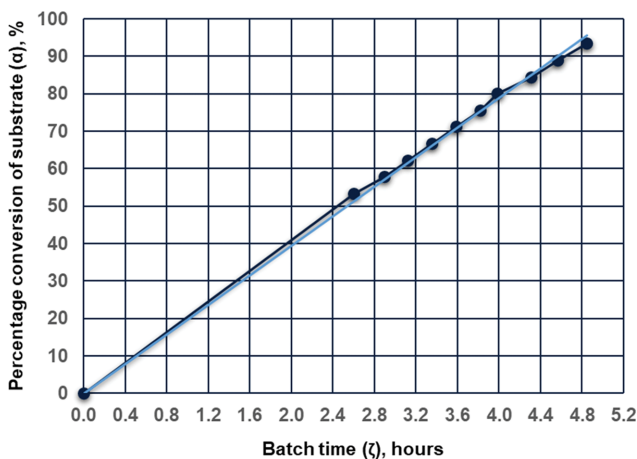


Fig. 9. Plot of fractional substrate conversion ( $\alpha$ ) versus batch time ( $\tau$ ) for batch, two phase MBBR with catalyst loading ( $\varepsilon$ )=0.015, support particle size ( $d_p$ )=1.0 mm.

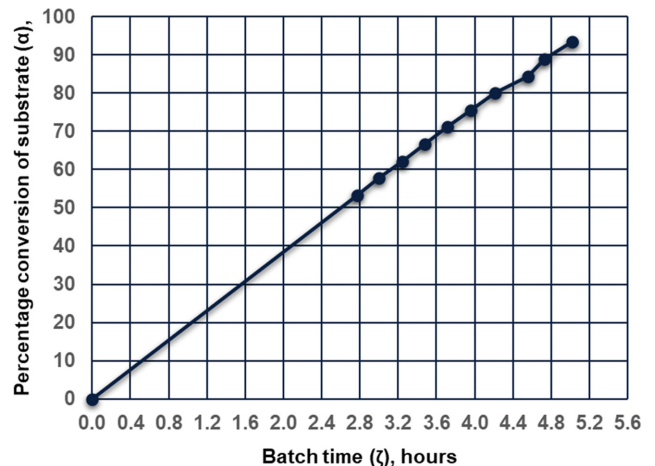


Fig. 11. Plot of fractional substrate conversion ( $\alpha$ ) versus batch time ( $\tau$ ) for batch, two phase MBBR with catalyst loading ( $\varepsilon$ )=0.02, support particle size ( $d_p$ )=2.0 mm.

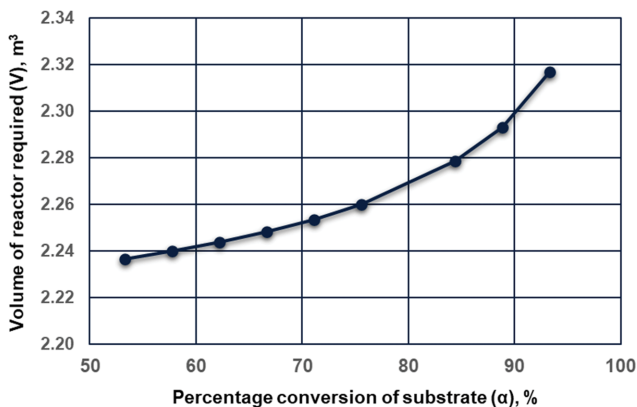


Fig. 10. Plot of volume of reactor required ( $V$ ) versus fractional substrate conversion ( $\alpha$ ) for batch, two phase MBBR with catalyst loading ( $\varepsilon$ )=0.015, support particle size ( $d_p$ )=1.0 mm.

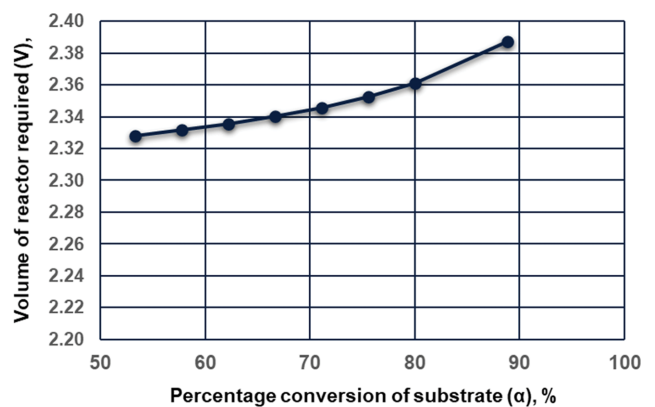


Fig. 12. Plot of volume of reactor required ( $V$ ) versus fractional substrate conversion ( $\alpha$ ) for batch, two phase MBBR with catalyst loading ( $\varepsilon$ )=0.02, support particle size ( $d_p$ )=2.0 mm.

such high impeller speed, the hydrodynamic shear generated will also be of high magnitude, which could tend to de-stabilize the biofilm.

The performance of an MBBR that employs larger size support particles such as  $d_p=2.0$  mm is illustrated in Figs. 11 and 12. Fig. 11 displays variation of fractional substrate conversion ( $\alpha$ ) with batch time ( $\tau$ ), while Fig. 12 illustrates how the volume of bioreactor required ( $V$ ) at  $M=100$  kg/d varies with  $\alpha$ . These plots are for  $\varepsilon=0.02$ . Here also, it can be noticed that  $\alpha$  varies almost proportionally with  $\tau$  ( $\alpha=0.1892 \tau$ ,  $R^2=0.9983$ ) and the variation of  $V$  with  $\alpha$ , and thereby with  $\tau$ , is marginal. However, at the same catalyst loading, when larger size support particles are used, longer batch time is required to attain the desired fractional conversion of lactose (Fig. 11). The volume of bioreactor required is also larger (Fig. 12). For example, for 80% conversion of lactose, the batch time required when  $d_p=1.0$  mm is 3.0 hours (Fig. 7), while with 2.0 mm support particles, a batch time as high as 4.2 hours is required to attain the same percentage conversion of lactose (Fig. 11). The volume of reactor required at  $M=100$  kg/d is about  $2.4 \text{ m}^3$  (Fig. 12), as compared to  $1.7 \text{ m}^3$  when  $d_p=1.0$  mm (Fig. 8).

This observation is understandable, since lower size particles possess larger specific surface and thereby facilitate substrate transfer and subsequent bioconversion in the biofilm. The bioreactor performance consequently gets improved. The operating cost of the bioreactor will also be higher with larger size support particles, since larger impeller speed and larger impeller power consumption become mandatory for keeping such large size particle-biofilm aggregates in suspension.

Another interesting observation is that the magnitude of effectiveness factor ( $\eta$ ) has been observed to be distinctly high (0.995 and higher) in all the cases, with both values of catalyst loading ( $\varepsilon$ ) and with both particle sizes. This indicates that the resistance to substrate transfer into the biofilm is quite low and, consequently, the rate of substrate transfer into the biofilm is significantly high.

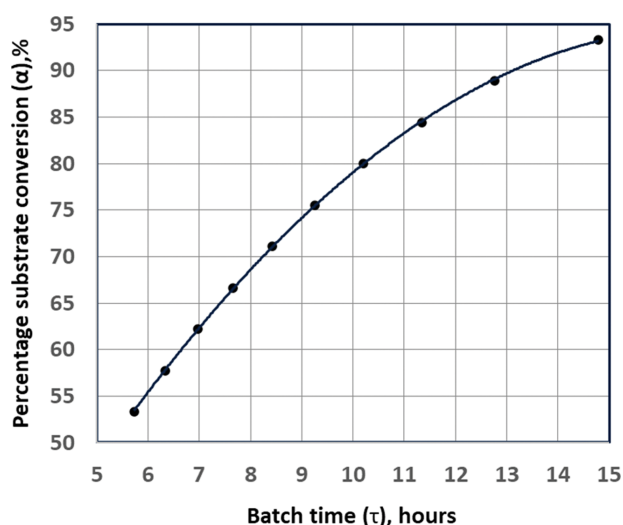


Fig. 13. Plot of fractional substrate conversion ( $\alpha$ ) versus batch time ( $\tau$ ) for batch, three phase MBBR (Xanthan gum production) with catalyst loading ( $X$ )=0.03,  $\varepsilon=0.0214$ , support particle size ( $d_p$ )=1.0 mm. Fractional gas holdup=0.07232.

This should be treated as an improved performance characteristic of these bioreactors.

### 3. Performance of Three Phase Batch MBBR (Xanthan Gum Production)

Typical performance characteristics of a batch, three phase moving bed biofilm reactor that handles Xanthan gum synthesis from cheese whey permeate are shown in Fig. 13. The case considered is that of a reactor employing 1.0 mm support particles, each surrounded by a thin film of *Xanthomonas campestris* culture, the mass fraction of catalyst particles (particle - biofilm aggregates) in the reaction mixture being 0.03 (the volume fraction,  $\varepsilon=0.0214$ ). This figure illustrates the variation of fractional substrate conversion ( $\alpha$ ) with batch time ( $\tau$ ), when the air flow rate is maintained at 7,200 L/hr (the fractional gas holdup at this flow rate having been estimated to be 0.07232). The variation of  $\alpha$  with  $\tau$  is only close to linear and a polynomial fit of second degree is seen to be best describing the  $\alpha - \tau$  dependence in this case:

$$\alpha = -0.336 \tau^2 + 11.285 \tau - 0.1614 \quad (R^2=0.999) \quad (49)$$

The data displayed in Fig. 13 demonstrate that the Xanthan gum synthesis from lactose (cheese whey permeate), apart from being aerobic, is a relatively slow process, as compared to lactic acid synthesis. This is evident from the fact that to achieve 80% conversion of lactose to Xanthan gum, a batch time of 10.2 hours is required (Fig. 13), while for bioconversion of lactose to lactic acid at the same catalyst loading ( $\varepsilon=0.02$ ) and with the same size of support particles ( $d_p=1.0$  mm), the batch time required is only 3.0 hours (Fig. 7).

However, Xanthan gum is a product that is not required to be manufactured in large tonnages per day since its use is mainly as an additive (stabilizing agent, emulsifying agent) in food, dairy and pharmaceutical industries, unlike lactic acid, which is the principal raw material for the manufacture of one of the most popular bioplastics such as PLLA (Poly Lactic Acid). As a result, a substrate conversion of 75%, and corresponding Xanthan gum yield,

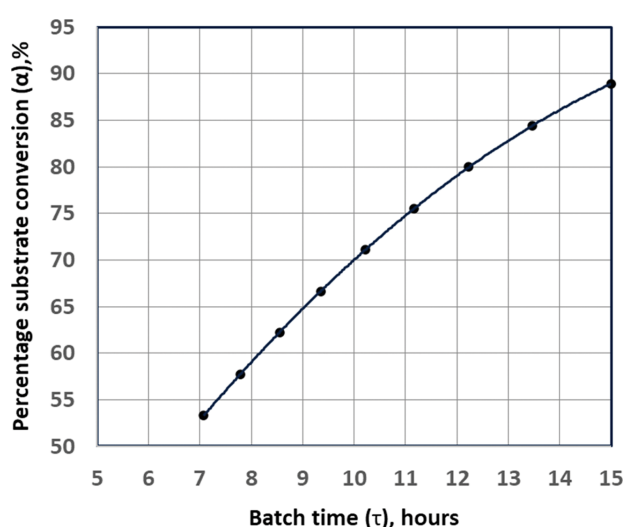


Fig. 14. Plot of fractional substrate conversion ( $\alpha$ ) versus batch time ( $\tau$ ) for batch, three phase MBBR (Xanthan gum production) with catalyst loading ( $X$ )=0.02,  $\varepsilon=0.015$ , support particle size ( $d_p$ )=1.0 mm. Fractional gas holdup=0.07183.

within 9.2 hours could be considered more less acceptable in the present case. This also speaks of the commercial possibility of using three phase batch MBBRs for Xanthan gum production.

The performance of a three phase MBBR that employs a lower catalyst concentration ( $X=0.02$ ) is shown in Fig. 14, once again in the form of a fractional substrate conversion ( $\alpha$ ) versus batch time ( $\tau$ ) plot. The reactor receives air at the same flow rate of 7,200 L/hr and this corresponds to a fractional gas holdup of 0.07183. Here also, the data fit into a second-order polynomial with reasonable accuracy ( $R^2=1.0$ ):

$$\alpha = -0.244 \tau^2 + 9.8817 \tau - 4.3863 \quad (R^2=1.0) \quad (50)$$

As can be seen from Fig. 14, when the catalyst concentration is low, the reactor requires a larger batch time to accomplish the same degree of substrate conversion. For example, at  $X=0.02$  ( $\varepsilon=0.015$ ), the batch time required to attain 75% conversion of lactose to Xanthan gum is 11.2 hours (Fig. 14), while within 9.2 hours at  $X=0.03$  (Fig. 13). In other words, the batch time requirement (processing time requirement) increases by 2.0 hours, when the mass fraction of catalyst particles in the reaction mixture is reduced from 0.03 to 0.02. This observation does not come as a surprise since this has been observed with lactic acid synthesis as well, but the increase in the batch time requirement is more pronounced in the present case.

Catalyst concentration is thus a detrimental parameter affecting the performance efficiency of the bioreactor. The change in the magnitude of  $X$ , however, has only marginal effect on the gas holdup. As stated earlier, too large concentration of particle-biofilm aggregates could favor inter-particle collisions and thereby tend to disturb the stability of the biofilm.

The dependence of particle size on bioreactor performance is illustrated in Fig. 15. This figure depicts the variation of fractional substrate conversion ( $\alpha$ ) with batch time ( $\tau$ ), when the reactor is being operated with 2.0 mm support particles. The mass fraction of particle-biofilm aggregates in the reaction mixture ( $X$ ) is main-

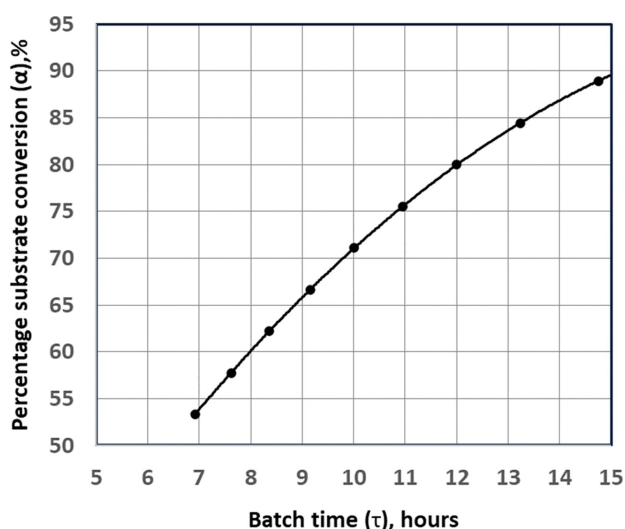


Fig. 15. Plot of fractional substrate conversion ( $\alpha$ ) versus batch time ( $\tau$ ) for batch, three phase MBBR (Xanthan gum production) with catalyst loading ( $X$ )=0.03,  $\varepsilon=0.017418$ , support particle size ( $d_p$ )=2.0 mm. Fractional gas holdup=0.072265.

tained at 0.03 ( $\varepsilon=0.017418$ ) and air is being sparged from the bottom at the same flow rate of 7,200 L/hr (estimated fractional gas holdup in the reactor=0.072265). In this case also, the data fit into a second-order polynomial (with  $R^2=1.0$ ) as given below:

$$\alpha = -0.2523 \tau^2 + 10.013 \tau - 3.8678 \quad (R^2=1.0) \quad (51)$$

The data presented in Fig. 15 ably demonstrate that by the use of larger size particles, which have lower specific surface, the reactor performance is degraded; and to achieve the desired degree of substrate conversion, the reactor is required to be operated for a larger period (larger batch time requirement). For example, the batch time (processing time) required to achieve 70% conversion of lactose to Xanthan gum is 10.0 hours with 2.0 mm particles (Fig. 15), while with 1.0 mm support particles, 70% conversion can be accomplished within 8.4 hours (Fig. 13) at the same value of catalyst concentration ( $X$ ). Thus, when the specific surface of particle - biofilm aggregates is reduced from 3,750  $m^2/m^3$  to 2,300  $m^2/m^3$  (by increasing  $d_p$  from 1.0 mm to 2.0 mm), the processing time requirement increases by around 2.0 hours. This observation is in agreement with that observed with two phase MBBR as well.

The magnitude of effectiveness factor ( $\eta$ ) has been observed to be of substantially high magnitude (more than 0.994) in this case of three phase operation of MBBR as well (true with both values of catalyst concentration ( $X$ ) considered and with both particle sizes). This brings to the conclusion that in three phase batch MBBRs also (in the case of aerobic operation as well), the resistance to substrate transfer into the biofilm is distinctly low.

#### 4. Continuous Operation of Two Phase MBBR (Lactic Acid Synthesis)

The continuous operation of two phase MBBR has been analyzed based on the tanks - in - series model described earlier, which was experimentally validated as discussed in the earlier section. The performance characteristics of such a continuous flow MBBR (dealing with synthesis of lactic acid from cheese whey permeate) are illustrated in Figs. 16-18. Fig. 16 illustrates the performance of a flow MBBR of volume 1.7  $m^3$  that employs 1.0 mm support par-

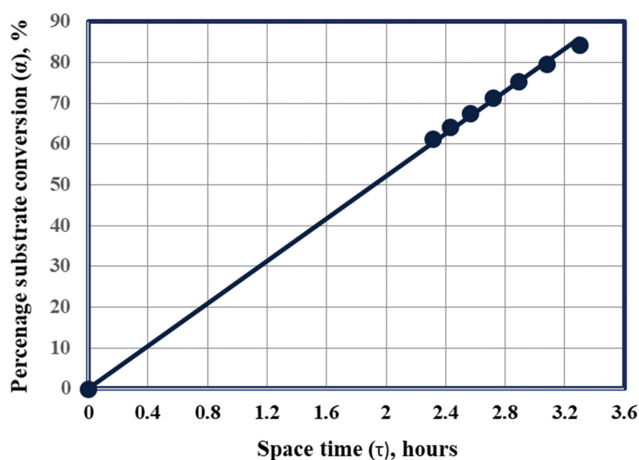


Fig. 16. Variation of fractional substrate conversion ( $\alpha$ ) with space time ( $\tau$ ) for continuous, flow MBBR (lactic acid synthesis, two phase operation) with catalyst loading ( $\varepsilon$ )=0.02, support particle size ( $d_p$ )=1.0 mm. Reactor volume=1.7  $m^3$ .

ticles (each surrounded by a thin film of *Lactobacillus helveticus* culture), the volume fraction of particle - biofilm aggregates in the reaction mixture ( $\varepsilon$ ) being maintained at 0.02. A graphical plot shown is that of fractional substrate conversion ( $\alpha$ ) versus space time ( $\tau$ ), where  $\tau$  for the bioreactor is defined as

$$\tau = [V(1 - \varepsilon)/Q_0] \quad (52)$$

As in the case of batch MBBR, the variation of  $\alpha$  with  $\tau$  is close to linear in the case of continuous operation as well and a regression analysis yielded the following relationship:

$$\alpha = 0.2608 \tau \quad (R^2 = 0.9989) \quad (53)$$

It can be seen from Fig. 16 that at  $\tau = 3.3$  hr, which corresponds to a feed flow rate of 500 L/hr, around 85% conversion of lactose to lactic acid is accomplished in this flow reactor, the rate of synthesis of lactic acid being around 97 kg/d. At higher capacities, at higher feed flow rates or lower values of space time  $\tau$ , the substrate conversion does get decreased and this is understandable since increase in feed flow rate causes decrease in the residence time of fluid elements in the reactor. However, since the substrate conversion ( $\alpha$ ) decreases almost proportionally with reactor space time ( $\tau$ ), the rate of production of lactic acid does not change materially with feed flow rate ( $Q_0$ ). As for example, at  $\tau = 2.3$  hr (feed flow rate = 720 L/hr), the conversion of lactose to lactic acid attained is 61%, the corresponding rate of lactic acid synthesis being around 100 kg/d. The rate of production of lactic acid thus remains more or less constant at 97 to 100 kg/d, even if the feed flow rate is increased from 500 to 720 L/hr. Also, this production rate is comparable to that achieved in a batch MBBR of same volume (discussed in Section 4.2). Two inferences can be arrived at based on these observations:

(a) The batch MBBR and the flow reactor provide comparable performance, both of them being of same volume,  $V$ . However, with the flow reactor continuous synthesis of lactic acid is possible, the production will not be in batches. Frequent shutting down and restarting of the bioreactor, at the end of each batch cycle, will not be required when the operation is continuous.

(b) Since the rate of production of lactic acid does not change materially with feed flow rate, it may be recommended that the bioreactor be operated at the lower flow rate of 500 L/hr since this would provide 85% conversion of lactose and, consequently, the product solution will contain less unconverted lactose and this will help in minimizing the cost of downstream processing.

As in the case of batch MBBR discussed earlier, in the case of continuous flow reactor also, the magnitude of effectiveness factor ( $\eta$ ) has been observed to be close to 1.0 at all feed flow rates. This has been found to be true with both particle sizes handled ( $d_p = 1.0$  mm, 2.0 mm) and at different values of catalyst loading ( $\varepsilon$ ) such as  $\varepsilon = 0.02$ , 0.015. Thus, in spite of being a heterogeneous system, the resistance to mass transfer into the catalyst particle (into the biofilm) is negligibly small in these reactors.

The performance of the flow reactor is significantly influenced by the catalyst loading ( $\varepsilon$ ). The reactor performance at a lower value of  $\varepsilon = 0.015$  is demonstrated in Fig. 17. The size of the support particles ( $d_p$ ) is maintained at 1.0 mm itself. Though the substrate conversion ( $\alpha$ ) increases with increase in space time,  $\tau$  with

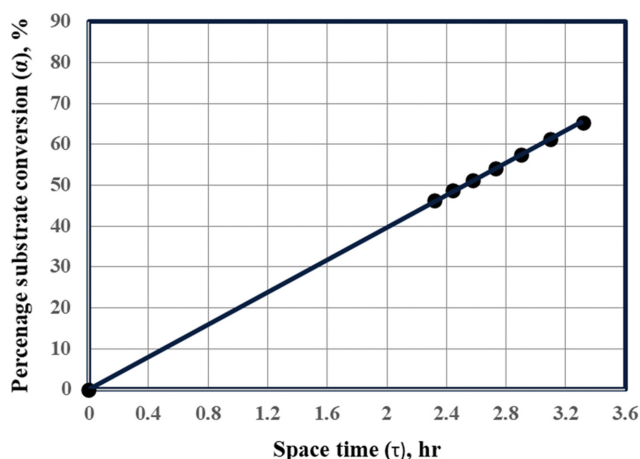


Fig. 17. Variation of fractional substrate conversion ( $\alpha$ ) with space time ( $\tau$ ) for continuous, flow MBBR (lactic acid synthesis, two phase operation) with catalyst loading ( $\varepsilon$ )=0.015, support particle size ( $d_p$ )=1.0 mm. Reactor volume=1.7 m<sup>3</sup>.

decrease in feed flow rate,  $Q_0$ , the substrate conversion attained at any specified value of feed flow rate, at any specified value of reactor space time, is significantly lower. For example, 61% conversion of lactose to lactic acid is attained at a feed flow rate of 540 L/hr (at  $\tau = 3.1$  hr) when the catalyst loading ( $\varepsilon$ ) is maintained at 0.015 (Fig. 17), while the same degree of substrate conversion can be achieved at a much higher capacity (feed flow rate) of 720 L/hr or at a much lower space time of 2.31 hr, when a higher catalyst loading of 0.02 is employed (Fig. 16). Alternately, at a specified space time of  $\tau = 3.1$  hr, the conversion of lactose to lactic acid decreases from 81% to 61% when the catalyst loading ( $\varepsilon$ ) is lowered from 0.02 to 0.015.

At  $\varepsilon = 0.015$  also, the variation of  $\alpha$  with  $\tau$  is more or less linear, such that they can be correlated as

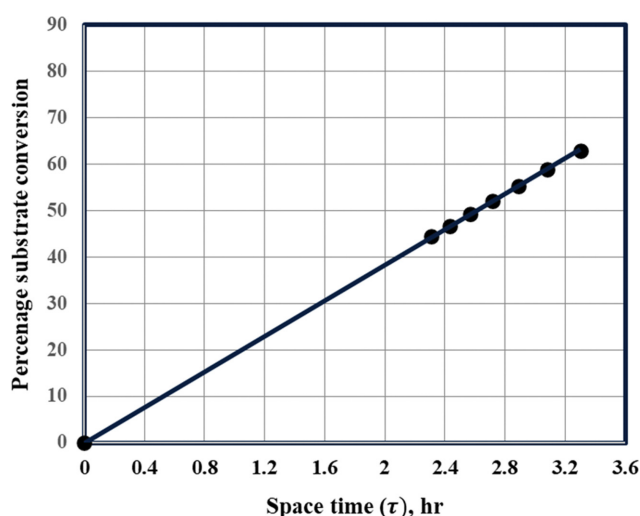


Fig. 18. Variation of fractional substrate conversion ( $\alpha$ ) with space time ( $\tau$ ) for continuous, flow MBBR (lactic acid synthesis, two phase operation) with catalyst loading ( $\varepsilon$ )=0.02, support particle size ( $d_p$ )=2.0 mm. Reactor volume=1.7 m<sup>3</sup>.

$$\alpha = 0.1983 \tau (R^2 = 0.9999) \quad (54)$$

As a consequence, the rate of production of lactic acid does not vary materially with feed flow rate in this case also and remains more or less constant at 74-75 kg/d. This value is around 25% lower than the rate of synthesis attained at  $\varepsilon = 0.02$ .

The specific surface of the catalyst particles (particle-biofilm aggregates) is a more influencing parameter as far as the continuous operation of the MBBR is concerned. This is evident from Fig. 18, which illustrates the  $\alpha - \tau$  relationship when the MBBR is operated with larger size support particles ( $d_p = 2.0$  mm), the catalyst loading ( $\varepsilon$ ) being maintained at the higher value of 0.02.

By comparing the data presented in Figs. 16 and 18, it can be observed that there is a significant reduction in the value of substrate conversion ( $\alpha$ ) when the particle size is increased from 1.0 mm to 2.0 mm. For example, at  $Q_0 = 540$  L/hr ( $\tau = 3.1$  hr), 80% conversion of lactose to lactic acid is achieved when 1.0 mm support particles are employed in the reactor (Fig. 16), but the substrate conversion gets reduced to 59% when the reactor is operated with 2.0 mm support particles, at the same flow rate or at the same space time. A decrease in specific surface by  $1,450$  m<sup>2</sup>/m<sup>3</sup> thus causes a 21% decrease in substrate conversion ( $\alpha$ ).

The  $\alpha - \tau$  relationship is close to linear in this case also:

$$\alpha = 0.1916 \tau (R^2 = 0.9999) \quad (55)$$

The rate of synthesis of lactic acid is lower (72-73 kg/d) and remains more or less constant irrespective of change in feed flow rate. As stated earlier, the  $\eta$  - values are close to unity even at higher particle size, such as  $d_p = 2.0$  mm, and also at lower values of catalyst loading such as  $\varepsilon = 0.015$ . This, no doubt, assists in improving the reactor performance.

### 5. Continuous, Three Phase Operation of MBBR (Xanthan Gum Production)

The continuous operation of three phase MBBR, dealing with Xanthan gum production from cheese whey permeate, was also analyzed mathematically using the tanks-in-series model and adequately substantiated through elaborate experimental data. As stated earlier, a CSTR-cascade consisting of three ideal CSTRs in series was observed to be equivalent to the MBBR under consideration. The performance characteristics of such a three phase MBBR that uses a catalyst loading ( $X$ ) of 0.03 (volumetric catalyst loading ( $\varepsilon$ ) = 0.0214) and 1.0 mm support particles (diameter of each particle-biofilm aggregate = 1.6 mm) are presented in Fig. 19. As in the case of three phase batch MBBR, in the case of this flow reactor also, the  $\alpha - \tau$  relationship follows a second-order polynomial fit as shown below:

$$\alpha = -0.3786 \tau^2 + 11.357 \tau (R^2 = 1.0) \quad (56)$$

Here, the reactor space time ( $\tau$ ) is defined as

$$\tau = [V(1 - \varepsilon - \varepsilon_0)/Q_0] \quad (57)$$

As can be seen from Fig. 19, Xanthan gum production from cheese whey permeate is a relatively slow process, analogous to that observed with batch MBBR, and as compared to lactic acid synthesis from the same raw material, which is a two phase process, Xanthan gum production demands larger space time (larger reactor volume or operation at lower feed flow rate) to attain the desired substrate

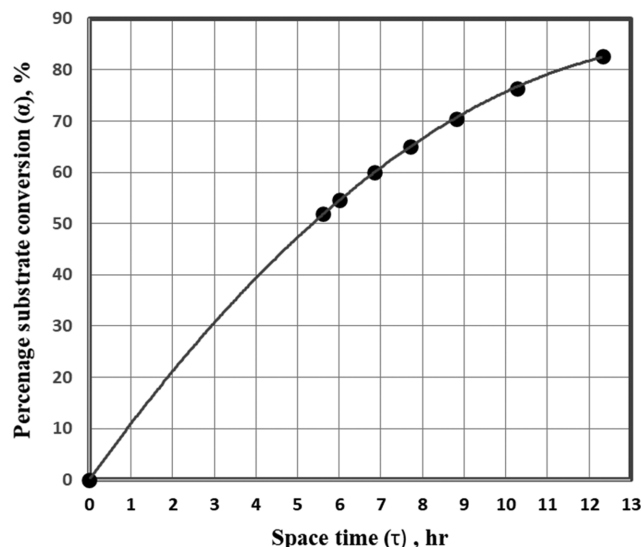


Fig. 19. Plot of fractional substrate conversion ( $\alpha$ ) versus space time ( $\tau$ ) for continuous, flow MBBR (three phase operation, Xanthan gum production) with catalyst loading ( $X$ ) = 0.03,  $\varepsilon = 0.0214$ , support particle size ( $d_p$ ) = 1.0 mm. Reactor volume =  $1.7$  m<sup>3</sup>.

conversion. As for example, 70.5% conversion of lactose to Xanthan gum is accomplished in a  $1.7$  m<sup>3</sup> reactor at a space time of 8.8 hours, at a feed flow rate of 175 L/hr, as shown in Fig. 19, but 71% conversion of lactose to lactic acid is possible in a bioreactor of same volume operating with a space time of only 2.7 hours, at a feed flow rate as high as 613 L/hr, as shown in Fig. 16. Note that both reactors are operating with 1.0 mm support particles and a catalyst loading ( $\varepsilon$ ) of 0.02-0.0214. No doubt, around 82% lactose conversion to Xanthan gum is obtained at a feed flow rate of 125 L/hr (space time = 12.3 hr) and 65% conversion at 200 L/hr in this reactor (Fig. 19), which cannot be labeled as unsatisfactory values of product yield, since as stated earlier, Xanthan gum is not required to be manufactured in large tonnages per day.

The value of effectiveness factor ( $\eta$ ) has been found to be substantially high (above 0.994) in three phase continuous operation as well, thereby confirming the high rate of substrate transfer into the biofilm existing in these reactors.

Three phase continuous operation at a lower value of catalyst loading such as at  $X = 0.02$  (correspondingly,  $\varepsilon = 0.015$ ) is illustrated in Fig. 20. The data fit into a second-order polynomial of following form :

$$\alpha = -0.2221 \tau^2 + 8.8114 \tau (R^2 = 1.0) \quad (58)$$

As anticipated from earlier cases, at a lower value of catalyst loading the bioreactor requires larger space time to provide the desired degree of lactose conversion. Conversely, at any specified space time, the fractional conversion of lactose attained is lower when the mass fraction of particle-biofilm aggregates in the reaction mixture ( $X$ ) is lower. For example 60% conversion of lactose to Xanthan gum is attained at a space time of around 8.9 hours, at a feed flow rate of 175 L/hr, when the reactor is operated with a catalyst loading of  $X = 0.02$  (Fig. 20), but the same percentage conversion of lactose

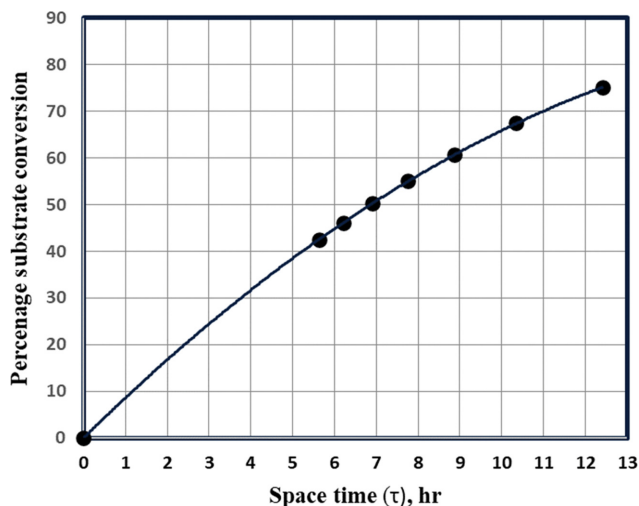


Fig. 20. Plot of fractional substrate conversion ( $\alpha$ ) versus space time ( $\tau$ ) for continuous, flow MBBR (three phase operation, Xanthan gum production) with catalyst loading ( $X$ )=0.02,  $\varepsilon$ =0.015, support particle size ( $d_p$ )=1.0 mm. Reactor volume=1.7 m<sup>3</sup>.

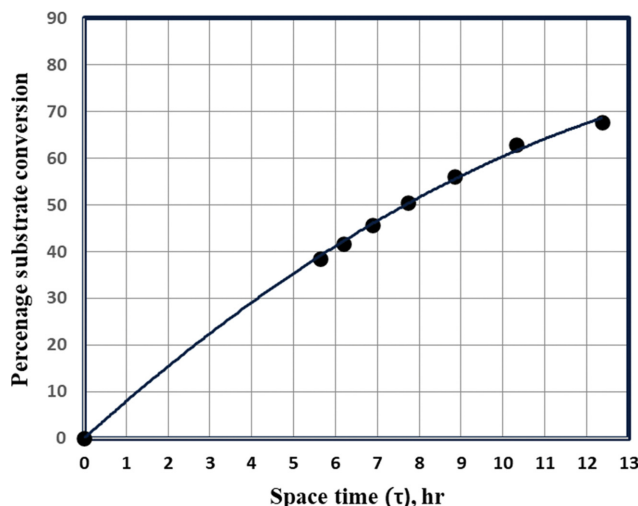


Fig. 21. Plot of fractional substrate conversion ( $\alpha$ ) versus space time ( $\tau$ ) for continuous, flow MBBR (three phase operation, Xanthan gum production) with catalyst loading ( $X$ )=0.03,  $\varepsilon$ =0.017418, support particle size ( $d_p$ )=2.0 mm. Reactor volume=1.7 m<sup>3</sup>.

could be achieved at  $\tau$ =6.8 hours (at  $Q_0$ =225 L/hr) if a larger catalyst loading of  $X$ =0.03 is maintained (Fig. 19). Conversely, at the same space time of  $\tau$ =8.9 hours, more than 70% conversion of lactose to Xanthan gum is possible at  $X$ =0.03 and the reactor is being operated at a large capacity (large feed flow rate) of 175 L/hr. To achieve the same conversion at  $X$ =0.02, the reactor would have to be operated at a lower feed flow rate (lower capacity or higher space time of about 11 hours). The value of fractional gas holdup ( $\varepsilon_g$ ) does not change materially due to decrease in the value of  $X$  or  $\varepsilon$ . This is once again as anticipated since the same has been observed in the case of three phase batch operation of MBBR as well.

Larger particle size and thereby lower specific surface of catalyst particles (particle-biofilm aggregates) also adversely affect the reactor performance in the case of three phase continuous operation as well. This is demonstrated by the ( $\alpha$ ) versus ( $\tau$ ) plot presented in Fig. 21. This plot corresponds to a support particle size ( $d_p$ ) of 2.0 mm (catalyst loading,  $X$ =0.03,  $\varepsilon$ =0.017418). In this case also, the variation fractional substrate conversion ( $\alpha$ ) with reactor space time ( $\tau$ ) could be represented by a second-order polynomial as given below:

$$\alpha = -0.2063 \tau^2 + 8.1012 \tau \quad (R^2 = 0.9988) \quad (59)$$

From Fig. 21, it can be seen that when larger size catalyst particles are used, only 56% conversion of lactose to Xanthan gum is obtained when the reactor is operated with a space time of 8.8 hours (feed flow rate=175 L/hr), while with 1.0 mm support particles, at the same reactor space time, around 70.5% conversion of lactose to Xanthan gum could be attained (Fig. 19). Even with a lower catalyst loading of  $X$ =0.02, 60.8% conversion of lactose is possible (Fig. 20) when 1.0 mm support particles are employed in the reactor. Specific surface of the catalyst particles (particle-biofilm aggregates) thus influences the reactor performance significantly.

The operation of the flow reactor does compare favorably with

that of three phase batch reactor (Section 4.3). For example, when the batch bioreactor is operated with 1.0 mm support particles and a catalyst loading of  $X$ =0.03, 71% lactose conversion is achieved within a batch time of 8.4 hours (Fig. 13), while the flow reactor provides 70.5% lactose conversion at a space time of 8.8 hours (Fig. 19). Similarly, during operation with a lower catalyst loading of  $X$ =0.02 and 1.0 mm support particles, the batch reactor provides 66.66% conversion of lactose to Xanthan gum in 9.5 hours of batch time (Fig. 14), which compares with the flow reactor providing 67% lactose conversion while operating with a space time of 10.2 hours (Fig. 20). Nevertheless, the tangible benefits of continuous operation such as the continuous output of the desired product without any intermittent shutdown or startup should have to be kept in mind while selecting between the two types of operation.

## CONCLUSIONS

Lactic acid synthesis (two phase process) and Xanthan gum production (three phase process) from cheese whey permeate in moving bed biofilm reactors (MBBRs) was studied. Xanthan gum synthesis is a relatively slower process as compared to lactic acid synthesis. In each case, the reactor performance is simulated mathematically and subsequently verified experimentally. These reactors exhibit promising characteristics when employed for low capacity installations. In the case of two phase batch MBBR and two phase continuous flow MBBR, the fractional substrate conversion ( $\alpha$ ) varies more or less linearly with batch time/space time ( $\tau$ ) and in the case of three phase operation, the  $\alpha$ - $\tau$  relationship follows a second-order polynomial. The magnitude of effectiveness factor ( $\eta$ ) is of high magnitude (more than 0.995) in these reactors. Reasonably high catalyst loading ( $\varepsilon$ =0.02,  $X$ =0.03) and lower size of catalyst particles (which corresponds to large specific surface) are preferred to achieve enhanced reactor performance.

## DECLARATIONS

## Funding

The authors have no relevant financial or non-financial interests to disclose. No funding has been received from any registered agency.

## Conflict of Interest

The authors have no conflict of interest to declare relevant to the contents of this article.

## Availability of Data and Material

The authors certify that they have no affiliations with or involvement in any organization or entity with any financial interest or non-financial interest in the subject matter or materials discussed in this manuscript. The authors also have no financial or proprietary interests in any material discussed in this article.

## NOMENCLATURE

$C_S$	: substrate concentration in liquid [g L <sup>-1</sup> ]
$C_{Se}$	: substrate concentration in product solution [g L <sup>-1</sup> ]
$C_{S0}$	: substrate concentration in feed solution [g L <sup>-1</sup> ]
$d_p$	: diameter of support particle [m]
$d_{pm}$	: diameter of particle-biofilm aggregate [m]
$D$	: diameter of reactor vessel [m]
$D_a$	: diameter of impeller [m]
$D_e$	: effective diffusivity of substrate into biofilm [m <sup>2</sup> s <sup>-1</sup> ]
$f$	: volume fraction of biofilm in particle-biofilm aggregate [m <sup>2</sup> m <sup>-3</sup> ]
$K_C$	: contois kinetic constant, dimensionless
$K_S$	: monod kinetic constant [g L <sup>-1</sup> ]
$L^*$	: characteristic dimension of particle-biofilm aggregate [m]
$n$	: speed of impeller [s <sup>-1</sup> ]
$P_{gl}$	: agitator power consumption for a gassed liquid [J s <sup>-1</sup> ]
$P_{glS}$	: agitator power consumption for three phase (gas-liquid-solid) system [J s <sup>-1</sup> ]
$P_L$	: agitator power consumption for an ungassed liquid [J s <sup>-1</sup> ]
$Q_g$	: volume flow rate of gas (air) [m <sup>3</sup> s <sup>-1</sup> ]
$Q_o$	: volume flow rate of feed solution [m <sup>3</sup> s <sup>-1</sup> ]
$(-r_o)(int)$	: intrinsic rate of bioconversion [g L <sup>-1</sup> s <sup>-1</sup> ]
$Re_m$	: mixing Reynolds number, dimensionless
$U_g$	: average superficial velocity of gas [m s <sup>-1</sup> ]
$V$	: V reactor volume [m <sup>3</sup> ]
$x$	: cell mass concentration [g L <sup>-1</sup> ]
$x_f$	: biomass (cell mass) concentration in biofilm [g L <sup>-1</sup> ]
$X$	: mass fraction of solids (particle - biofilm aggregates) in the reaction mixture
$Y$	: overall yield coefficient for cell mass production [g g <sup>-1</sup> ]
$\alpha$	: fractional conversion of substrate, dimensionless
$\beta$	: parameter defined in Eq. (14) and in Eq. (33), dimensionless
$\delta$	: biofilm thickness [m]
$\varepsilon$	: volume fraction of particle - biofilm aggregates in the reaction mixture, dimensionless
$\varepsilon_g$	: fractional gas holdup in reaction mixture, dimensionless
$\eta$	: effectiveness factor, dimensionless
$\mu_L$	: liquid viscosity [kg m <sup>-1</sup> s <sup>-1</sup> ]

$\mu_m$	: maximum specific growth rate [s <sup>-1</sup> ]
$\rho_L$	: liquid density [kg m <sup>-3</sup> ]
$\rho_m$	: density of microbial solution [kg m <sup>-3</sup> ]
$\rho_S$	: density of support particle [kg m <sup>-3</sup> ]
$\rho_{Sm}$	: density of particle - biofilm aggregate [kg m <sup>-3</sup> ]
$\tau$	: space time; batch time [s]
$\emptyset$	: Thiele-type modulus, dimensionless

## REFERENCES

1. H. Ødegaard, *Water Sci. Technol.*, **42**, 33 (2000).
2. J. P. Mcquarrie and J. P. Boltz, *Water Environ. Res.*, **83**, 560 (2011).
3. B. Rusten, E. Mattsson, A. B. Due and T. Westrum, *Water Sci. Technol.*, **30**, 161 (1994).
4. L. J. Hem, B. Rusten and H. Ødegaard, *Water Res.*, **28**, 1425 (1994).
5. B. Rusten, L. J. Hem and H. Ødegaard, *Water Environ. Res.*, **67**, 75 (1995).
6. M. Maurer, C. Fux, M. Graff and H. Siegrist, *Water Sci. Technol.*, **43**, 337 (2001).
7. B. Rusten, L. J. Hem and H. Ødegaard, *Water Environ. Res.*, **67**, 65 (1995).
8. B. Szatkowska, G. Cema, E. Plaza, J. Trela and B. Hultman, *Water Sci. Technol.*, **55**, 19 (2007).
9. M. Kermani, B. Bina, H. Movahedian, M. M. Amin and M. Nikaein, *Am. J. Environ. Sci.*, **4**, 675 (2008).
10. M. Kermani, B. Bina, H. Movahedian, M. M. Amin and M. Nikaein, *Iranian J. Biotech.*, **7**, 18 (2009).
11. S. Chen, D. Z. Sun and J. S. Chung, *Waste Manage.*, **28**, 339 (2008).
12. B. P. Sahariah, J. Anandkumar and S. Chakraborty, *Desalin. Water Treat.*, **57**, 14396 (2016).
13. J. Anandkumar, A. Yadu and B. P. Sahariah, *J. Mod. Chem. Chem. Technol.*, **7**, 37 (2016).
14. C. M. Narayanan, *Int. J. Chem. Eng. Proc.*, **1**, 1 (2015).
15. C. M. Narayanan and S. Das, *Adv. Chem. Eng. Sci.*, **6**, 130 (2016).
16. C. M. Narayanan and S. Das, *Int. J. Environ. Waste Manage.*, **19**, 1 (2017).
17. A. Pandey and C. M. Narayanan, *Int. J. Trans. Phenom.*, **14**, 241 (2017).
18. C. M. Narayanan, S. Das and A. Pandey, in *Handbook of food bio-engineering - Volume 2*, A. M. Grumezescu and A. M. Holban Eds, Academic Press, London (2017).
19. C. M. Narayanan, *Chem. Prod. Process Model.*, **10**, 55 (2015).
20. A. W. Schepers, J. Thibault and C. Lacroix, *Enzyme Microbial Tech.*, **30**, 176 (2002).
21. J. C. Gottifredi and E. E. Gonzo, *Chem. Eng. J.*, **109**, 83 (2005).
22. N. Dohi, Y. Matsuda, N. Itano, K. Shimizu, K. Minekawa and Y. Kawase, *Chem. Eng. Commun.*, **171**, 211 (1999).
23. Y. Bao, Z. Hao, Z. Gao, L. Shi, J. M. Smith and R. B. Thorpe, *Chem. Eng. Commun.*, **193**, 801 (2006).
24. A. K. Rapala and J. Karcz, *Chem. Papers*, **64**, 154 (2010).
25. A. K. Rapala and J. Karcz, *Chem. Papers*, **66**, 574 (2012).
26. M. M. Godlewska and J. Karcz, *Chem. Papers*, **66**, 566 (2012).
27. A. J. Patrick and M. J. Kennedy, *Biotech. Lett.*, **17**, 487 (1995).
28. G. L. Zabot, J. Mecca and M. Mesomo, *Bioprocess Biosyst. Eng.*, **34**, 975 (2011).